Reflectance Infrared Spectroscopic Analysis of Polymers at the Air−Water Interface. 4. Microstructure of Poly(dimethylsiloxane)

Thomas D. Hahn and Shaw Ling Hsu*

Polymer Science and Engineering Department and Materials Research Science and Engineering Center, University of Massachusetts, Amherst, Massachusetts 01003

Howard D. Stidham

Chemistry Department, University of Massachusetts, Amherst, Massachusetts 01003

Received July 26, 1996; Revised Manuscript Received October 21, 1996[⊗]

ABSTRACT: At room temperature, monolayer films of poly(dimethylsiloxane) spread on the air−water interface display nearly constant surface pressures in the region between surface concentrations of 0.75 and 1.6 mg/m^2. Studies of these films in this region by epifluorescence microscopy and external reflectance infrared spectroscopy are reported. Two surface phases were detected by the epifluorescence micrographs. The infrared reflectance spectra in the 1000−1100 cm^{-1} region and at concentrations between 0.75 and 1.6 mg/m^2 can be fit as a mixture of infrared features observed at these surface concentration limits. At 0.75 mg/m^2, the infrared reflectance data are consistent with a random chain in which the oxygen atoms are largely exposed to the water surface, described by earlier workers as a twisted caterpillar, or a two-dimensional random coil with as many oxygen atoms as possible exposed to water. At 1.6 mg/m^2, the infrared data indicate that the oxygen atoms are largely excluded from contact with water and suggest the presence of a more ordered structure consistent with helical segments which have the helix axis parallel to the water surface.

Introduction

Surface pressure versus surface area or surface concentration isotherms of poly(dimethylsiloxane) spread on water have been studied since at least 1947.[1] The general features of the isotherm are well-known.[2−10] Upon compression the isotherm begins at zero surface pressure at surface concentrations significantly below 0.75 mg/m^2. Around $\Gamma_1 \approx 0.75$ mg/m^2, the surface pressure π jumps substantially to about 9 mN/m, where it exhibits a plateau until about $\Gamma_2 \approx 1.6$ mg/m^2, where a small π jump occurs followed by a smaller rise. Oligomers with strongly adsorbing end groups may also show other transitions.[6] Structural features associated with the various transitions have often been debated. Particular controversy has arisen over the structural features associated with the π plateau around 9 mN/m between Γ_1 and Γ_2.[4,7,8]

Fox and co-workers constructed possible structures at the various transition points by using molecular models with tetrahedral geometry.[1] At low surface pressures, these workers suggested a caterpillar-like structure with all the oxygens in the water, and all the methyl groups pointing away from the water surface. The structure becomes considerably twisted with an initial jump in surface pressure. Compression in the surface pressure plateau around 9 mN/m corresponds to a molecular transformation from the twisted caterpillar-like structure to a helix with the helix axis parallel to the water surface. Noll et al.[10] proposed similar structures in the π plateau region, and the caterpillar structure was suggested as the structure that adsorbs to galena in ore flotation. Thermodynamic studies of Granick and co-workers have suggested that linear and large cyclic poly(dimethylsiloxane) chains undergo similar transitions in the region of the π plateau.[3] Granick et al. also stated that a negative temperature coefficient of π suggests that decreasing the surface area of poly(dimethylsiloxane) films in the plateau region corresponds to a slight surface entropy increase. Characterization of the isotherm with damping of capillary waves supports an exchange between two structures in the vicinity of the π plateau.[2] Lenk and co-workers[6] have also pointed out that, due to the bond angle differences along the backbone with Si−O−Si ∼145°, and O−Si−O ∼ tetrahedral, an extended chain structure cannot persist for very many units without leaving the water surface, or twisting of the backbone. Mann and Langevin attempted to characterize the isotherm with Brewster angle ellipsometry.[7] Lee, Mann, Langevin, and Farnoux extended the work of Mann and Langevin with small angle neutron scattering,[4] and Mann, Henon, Langevin, and Meunier extended their work further with Brewster angle microscopy.[8] Collectively, these three papers were unable to explain the π plateau between Γ_1 and Γ_2 and also questioned the coexistence of two structures in this region.

It is the intent of this report to present a study of the microstructural features of poly(dimethylsiloxane), $CH_3-[Si(CH_3)_2-O]_n-Si(CH_3)_3$, spread at the air−water interface in the vicinity of the π plateau at 9 mN/m. Epifluorescence microscopy has been used in the past to illustrate the coexistence of two phases in the vicinity of a surface pressure plateau.[11−13] In addition, poly(dimethylsiloxane) spread at the air−water interface is characterized by external reflectance infrared spectroscopy.

Experimental Section

Poly(dimethylsiloxane) of $M_w = 37\,000$ and $M_w/M_n = 1.6$ was purchased from United Chemical Technologies, Inc., and was used as supplied. The fluorescent probe 1-palmitoyl-2-[12-[(7-nitro-2,1,3-benzoxadiazol-4-yl)amino]hydroxydecyl]phosphatidylcholine NBD-PC was purchased from Avanti Polar Lipids

* To whom correspondence should be addressed.

[⊗] Abstract published in *Advance ACS Abstracts,* December 15, 1996.

S0024-9297(96)01122-9 CCC: $14.00

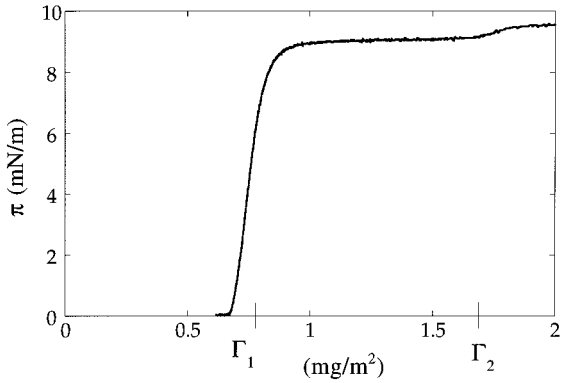

Figure 1. Poly(dimethylsiloxane) isotherm on water.

and was used as supplied in 1 mg/mL chloroform solution. All solutions of poly(dimethylsiloxane) were prepared using spectroscopic grade dichloromethane as solvent.

Isotherm experiments were conducted on a commercial NIMA type 611 Langmuir−Blodgett trough on deionized water. Water surface purity was established by compressing the barriers and aspirating the surface until no surface pressure change accompanied further compression or expansion. All samples were spread on water from solutions of concentrations near 20 mg/100 mL and were allowed to stand at least 15 min to assure complete evaporation of solvent. Surface pressure measurements were made with a filter paper Wilhelmy plate suspended from an electrobalance.

Micrographs of poly(dimethylsiloxane) spread on water from 3.26 mg/mL solution in dichloromethane containing 0.0196 mg/mL NBD-PC were obtained using a Zeiss Axioplan epifluorescence microscope equipped with a 1.6× camera eyepiece and a 32× objective focused on the air−water interface in a Langmuir trough specifically constructed to fit the microscope stage. Light from a Xenon lamp source is passed through a band pass filter that selects 450−490 nm radiation, followed by a dichroic mirror which reflects wavelengths shorter than 510 nm and passes wavelengths longer than 510 nm. The reflected light passes through the objective and is focused on the water surface. Fluorescence centered near 534 nm is excited by the focused light near 460 nm, returns through the objective, and is passed by the dichroic mirror. A long pass filter with a cutoff at 520 nm is set above the dichroic mirror to block scattered light. The fluorescent image is then focused on a Genisys microchannel plate photomultiplier manufactured by Dage MTI, from which a thermal print is made.

External reflectance infrared spectra were obtained with a Perkin-Elmer system 2000 FTIR equipped with a Specac Langmuir trough reflectance attachment purchased from Specac Ltd., operated with s polarization at 30° angle of incidence. Resolution was set at 4 cm^{-1}, and 2048 scans were co-added to obtain the background, 100%, and sample spectra of infrared radiation reflected at the air−water interface in the trough. The surface of deionized water was compressed as far as possible and aspirated several times at the beginning of each run to achieve maximum surface cleanliness. Poly(dimethylsiloxane) samples were typically spread from solution concentrations approximately 20 mg/100 mL in spectroscopic grade dichloromethane and allowed to set at least 15 min before the sample spectra were collected.

Results and Discussion

Figure 1 shows a typical isotherm for poly(dimethylsiloxane) film cast on a water surface. At surface concentrations less than $\Gamma_1 \approx 0.75$ mg/m^2, π is essentially zero. Near this concentration, π rises sharply to about 9 mN/m and remains at this value between Γ_1 and $\Gamma_2 \approx 1.6$ mg/m^2. At Γ_2, the surface pressure again rises slightly and then increases very slowly thereafter.

Figure 2 shows bright and dark domains in a typical fluorescence micrograph for poly(dimethylsiloxane) spread on water in the plateau region at a surface concentration

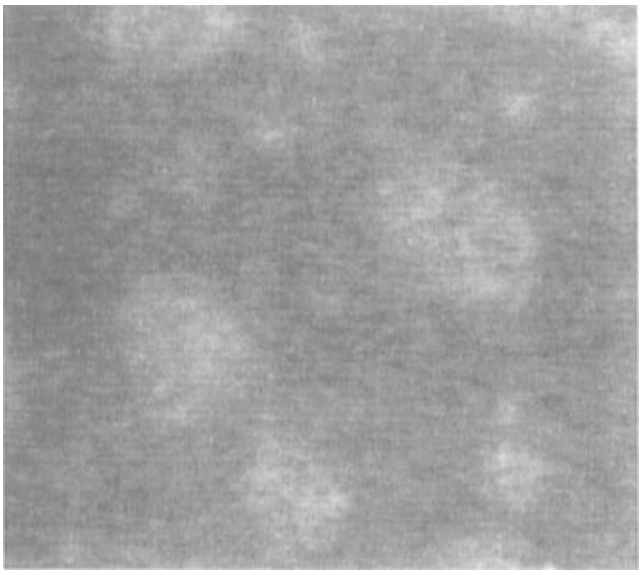

Figure 2. Epifluorescence microscopy micrograph for poly(dimethylsiloxane) film spread on water at 1.1 mg/m^2, with 0.6% by weight probe on polymer.

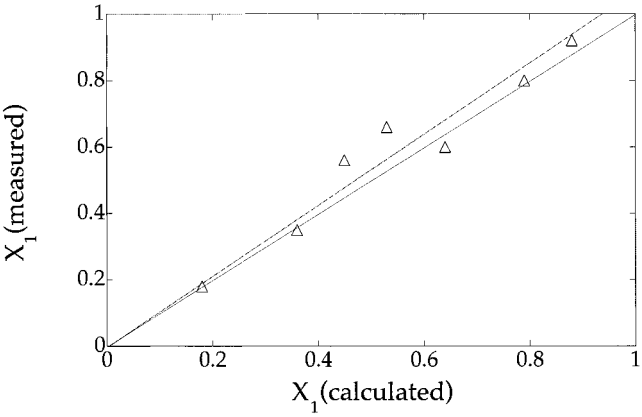

Figure 3. Lever rule calculated and microscopy measured component fraction of Γ_1 structure between concentrations Γ_1 and Γ_2. The theoretical slope of this curve is 1 (solid line), while the calculated slope (dashed line) is 0.94 ± 0.1 (standard deviation). Deviation from X_1(measured) for X_1(calculated) is likely due to uncertainty in the relative area measurements, although uncertainty in Γ_1 and Γ_2 may also contribute.

between Γ_1 and Γ_2. Upon further compression, the bright domains increase at the expense of the dark domains, providing evidence for the coexistence of two distinct surface structures. The relative areas of the bright and dark domains may be measured, and the fraction X of the area that is dark may be calculated. The fraction may also be calculated from the average surface concentration Γ by assuming a linear response

$$X = \frac{\Gamma - \Gamma_2}{\Gamma_1 - \Gamma_2} \tag{1}$$

Figure 3 shows a plot of X calculated from the light and dark areas of a micrograph against X calculated from the linear assumption. The linear behavior of this plot strongly suggests a progression between two distinctive structures in the plateau region between Γ_1 and Γ_2. Since Γ_2 is 2.13 times as great as Γ_1, the film thickness at Γ_2 is probably about twice that at Γ_1, provided the film bulk density is not too different at the two concentrations.

External reflectance infrared spectroscopy provides further evidence for the coexistence of two structures

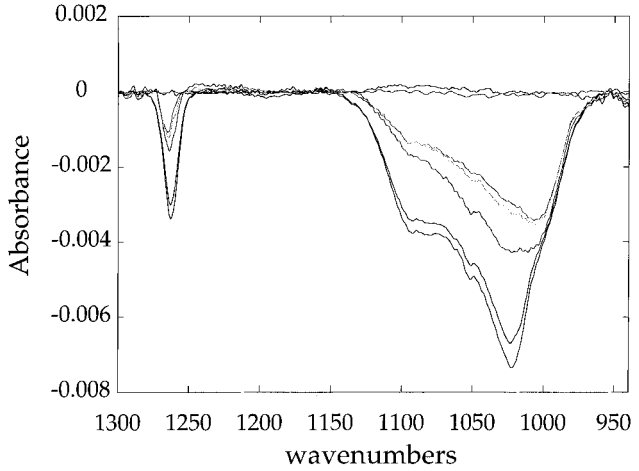

Figure 4. External reflectance infrared spectra for poly(dimethylsiloxane) film spread on water at several concentrations between Γ_1 and Γ_2.

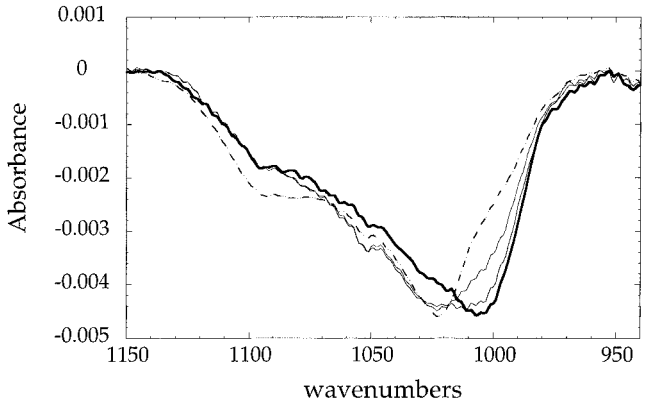

Figure 5. Scaled external reflectance infrared spectra of the ν_{as} band for poly(dimethylsiloxane) film spread on water at several concentrations between Γ_1 and Γ_2.

in the plateau region between Γ_1 and Γ_2 and suggests that the structure at Γ_2 is more ordered. Representative external reflectance infrared spectra are displayed in absorbance mode in Figure 4, together with a 100% line for reference. The broad band in the 1000−1100 cm^{-1} region has been assigned to the asymmetric Si−O−Si stretching mode by several authors,[14,15] and the sharp band centered at 1264 cm^{-1} to the symmetric methyl deformation, consistent with the early suggestion of Wilmshurst.[16]

A broad band containing several components is found in the 1000−1100 cm^{-1} region. The features of the band change significantly as the surface concentration is varied between Γ_1 and Γ_2. At Γ_1 the most intense band is at 1005 cm^{-1}. At Γ_2, the most intense peak occurs at 1020 cm^{-1}. Weaker components are found around 1055 and 1090 cm^{-1}. All components persist to some extent at all concentrations studied. In Figure 5, the 1000−1100 cm^{-1} region is plotted with all spectra normalized by division by the corresponding surface concentration. These spectra suggest that the 1020 cm^{-1} band originates in one structure and the 1005 cm^{-1} band in another. Konopka and Stojczyk[17] found that the frequency of the asymmetric Si−O−Si stretching vibration varies in solvents of varying dielectric constants and dipole moments and showed that in many cases the frequency shifts to lower values with increasing dielectric constant in accordance with the theoretical model due to Kirkwood, Bauer, and Magat.[18] Some cases proved better described by the later model of Allerhand and von Schleyer.[19] The dielectric constant of water is one of the highest known, and the observations of Konopka and Stojczyk suggest that Si−O−Si linkages in aqueous surroundings should usually be expected to display shifts in the asymmetric stretching frequency of the order of 15 cm^{-1} relative to the frequency of the group in surroundings of much lower dielectric constant. These expectations are consistent with the observations shown in Figures 4 and 5, the low frequency of 1005 cm^{-1} suggesting contact of the Si−O−Si groups with water in reflectance spectra obtained at low surface concentrations.

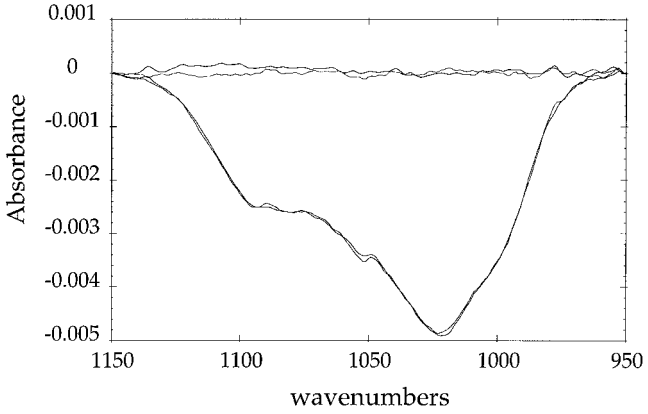

Figure 6. Measured and constructed spectra at $X_1 = 0.58$, for the band described in Figure 5.

The external reflectance infrared spectrum obtained for each surface concentration can be represented as a linear combination of absorbances of the constituents measured at each frequency. If $A_\nu(\Gamma)$ is the composite absorbance value at surface concentration Γ at a frequency ν, while $A_\nu(\Gamma_1)$ is the absorbance at ν for Γ_1 and similarly $A_\nu(\Gamma_2)$ is that for Γ_2, the composite spectrum may be constructed by superposing the contributors at each frequency as

$$A_\nu(\Gamma) = XA_\nu(\Gamma_1) + (1 - X)A_\nu(\Gamma_2) \quad (2)$$

The composite spectrum $A_\nu(\Gamma)$ synthesized in this way can then be plotted against the observed spectrum $A_\nu(\Gamma)_{exp}$ initially for the value of X with which the trough was charged. Although $A_\nu(\Gamma_1)$ and $A_\nu(\Gamma_2)$ are only available experimentally, and each of these two spectra contain evidence of traces of the dominant constituent in the other, fairly good empirical fits can be made by least squares procedures that minimize the squares of the residuals at each frequency. The residual r_ν at ν is

$$r_\nu(X) = A_\nu(\Gamma)_{exp} - [XA_\nu(\Gamma_1) + (1 - X)A_\nu(\Gamma_2)] \quad (3)$$

and X is varied to produce a minimum in the sum of the squared residuals, the sum running over all the points sampled in the frequency interval. A comparison of one such fitted spectrum with a measured spectrum is shown in Figure 6. Similar fits were obtained for other surface concentrations between Γ_1 and Γ_2. A comparison between values of X obtained from eq 1 and the value of X used to fit the corresponding spectrum is shown in Figure 7. The scatter in the data is large due to uncertainty in the measurement of Γ_1, Γ_2, and Γ used to calculate X, but the slope of 0.9 ± 0.1 is consistent with the fluorescence microscopy observation of two coexistent surface phases in the plateau region between Γ_1 and Γ_2.

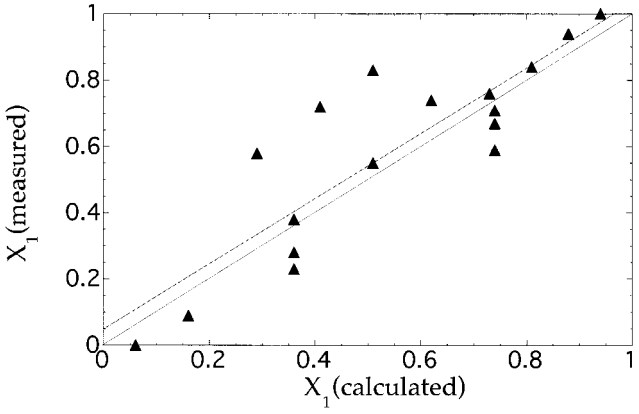

Figure 7. Lever rule calculated and infrared measured component fraction of Γ_1 structure between concentrations Γ_1 and Γ_2. The calculated slope is 0.98 ± 0.15. See Figure 3 for details.

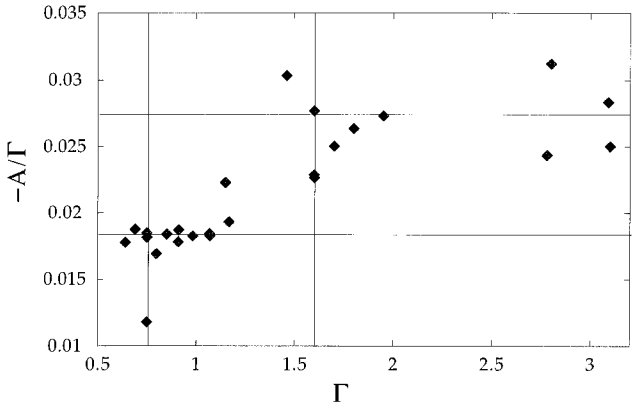

Figure 8. Absorbance divided by surface concentration versus surface concentration for the orientation sensitive band at 1264 cm^{-1}, as described in the text.

Figure 4 shows that the 1264 cm^{-1} band does not shift in frequency as surface concentration is changed and that there is no observable splitting into several components. Figure 8 shows that when the integrated peak absorbance of this band is divided by surface concentration and then plotted against surface concentration, the absorbance/concentration ratio is not constant. The plot jumps between extreme values at the limiting surface concentrations Γ_1 and Γ_2. Reference to Figure 9 shows that the symmetric methyl deformation must have two components whose transition moments lie in the C−Si−C plane, one parallel to the angle bisector, and the other perpendicular to it. If the structure of the poly(dimethylsiloxane) molecules in the surface film at Γ_1 is one in which the hydrophobic methyl groups are as far from the air−water interface as possible while the hydrophilic O−Si−O groups are attracted to the water surface, the plane containing the C−Si−C group will tend to be perpendicular to the water surface. Spectra obtained with s polarization will then be predominantly sensitive to the components represented by the intersection between the planes of C−Si−C and water. If there is a helical structure that occurs in the phase at Γ_2, many of the planes containing C−Si−C groups have some angle significantly different from perpendicular to the water surface. Thus, the transition moments in the C−Si−C plane will tend to have projections onto the water surface greater than those at Γ_1. Figure 8 thus indicates that segmental orientation is different at the two extremes of surface concentration and that the intrinsic intensity of the 1264 cm^{-1} band can be used

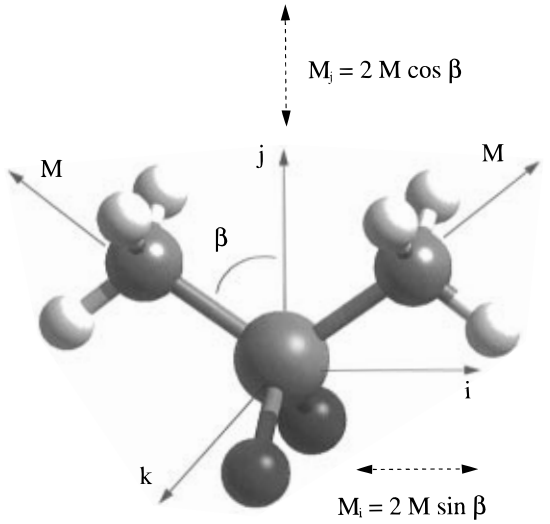

Figure 9. Transition moments for the band at 1264 cm^{-1}, as described in the text.

to provide a measure of the origin of the difference. The following is an account of our attempt to make these qualitative considerations more quantitative.

The calculation starts by projecting one transition moment $M_i = 2M \sin(\beta)$ for the out-of-phase symmetric deformation onto the laboratory x axis. For simplicity, the in-phase and out-of-phase deformations are represented using the same moment M, related to the transition moment for an isolated methyl group. The laboratory x axis is defined by the electric vector of the incident light. Since only s polarization was used, the x axis lies in the plane of the air−water interface. The projected transition moment $M_{x,i}$ is

$$M_{x,i} = M_i \sin(\gamma) \cos(\phi) \tag{4}$$

The average absorbance for transition moment M_i can be represented as

$$A_{x,i} = \int_0^{2\pi} \int_0^{\pi} a(\gamma,\phi) M_{x,i}^2 \sin(\gamma)\, d\gamma\, d\phi \tag{5}$$

where $a(\gamma,\phi)$ is a distribution function.[20] Since the in-phase and out-of-phase deformations are accidentally degenerate, there are two transition moments for each monomer segment at the same frequency. The calculation of the in-phase symmetric deformation absorbance is as above, with the replacement of $A_{x,i}$ with $A_{x,j}$, $M_{x,i}$ with $M_{x,j}$, and M_i with $M_j = 2M \cos(\beta)$. Since there is no component perpendicular to the C−Si−C plane for these vibrations, $M_k = 0$ and the total is the sum of the averaged contributions

$$A_x = A_{x,i} + A_{x,j} \tag{6}$$

For totally random orientation, $a(\gamma,\phi)$ is a constant. Since only ratios are involved in the interpretation, for simplicity $a(\gamma,\phi) = a$ is normalized to unity by writing

$$\int_0^{2\pi} \int_0^{\pi} a \sin(\gamma)\, d\gamma\, d\phi = 1 \tag{7}$$

The result for random orientation is then

$$A_x = \frac{2}{3} M^2 \tag{8}$$

If one of the three axes i, j, or k is constrained to be perpendicular to the air−water interface, the absor-

Table 1. Measured Absorbances and Calculated Absorbances for Different Structures

structure	absorbance A/Γ
$A(\Gamma_1)$	0.017
$A(\Gamma_2)$	0.026
$A(\Gamma_2)/A(\Gamma_1)$	1.5
isotropic	$^2/_3M^2$
extend chains, all trans and linear:	
perpendicular to water surface	$2M^2$
parallel to water surface	$0.66 - 1.34M^2$
twisted caterpillar[a]	$1M^2$
helical structure:	
helix axis perpendicular to water surface	$1.22M^2$
helix axis parallel to water surface	$1.34 - 1.45M^2$

[a] This value would be the average of the absorbance values with the chain parallel to the water surface. The same absorbance value would also be measured for the 2-D random walk, assuming that the chain axis for each monomer is strictly confined to be in the *xy* plane.

bance calculation involves only the plane angle ϕ. For the ith component,

$$A_{x,i} = \int_0^{2\pi} a(\phi) M_{x,i}{}^2 \, d\phi \tag{9}$$

The surface is assumed to be isotropic, and $a(\phi) = a$ is a constant. As above, $a(\phi)$ is normalized to unity, the condition for which is

$$\int_0^{2\pi} a \, d\phi = 1 \tag{10}$$

In this case, $M_{x,i} = 0$ if the i axis is normal to the surface, but $M_{x,i} = M_i \cos\phi$ if the i axis is in the *xy* plane. There are three cases. If the k axis is normal to the plane, both the i and j axes lie in the plane and contribute to the total absorbance. The result is exactly $A_x = 2M^2$. However, if the j axis is perpendicular to the plane, only the i axis contributes, and the result is $A_x = 2M^2 \cos^2\beta$, while if the i axis is perpendicular to the plane, only the j axis contributes and the result is $A_x = 2M^2 \sin^2\beta$. When $\beta \approx 55°$ is used for a tetrahedral geometry, the result is $0.66M^2$ or $1.34M^2$. These results would be applicable to models involving the all-trans silicon−oxygen chain perpendicular to the air−water interface ($2M^2$), or lying flat on the surface with the j axis in the *xy* plane ($0.66M^2$) or with the i axis in the *xy* plane ($1.34M^2$), depending on how the chain was rotated about the long axis. These results are summarized in Table 1.

In the twisted caterpillar model, the chain axis, which is the k axis at each monomer unit, lies in the *xy* plane, and the j and i axes can have any orientation relative to the surface normal. If M_i and M_j are oriented randomly with respect to the normal to the surface, each contributes equally and the average absorbance A_x is just M^2.

The crystal structure of poly(dimethylsiloxane) has been reported by Damaschun to exhibit C_2 symmetry, with six repeating monomer units per cell.[21] This structure is taken as representative of short helical segments that may form in the more compressed film at surface concentration Γ_2. To obtain the atomic coordinates, the suggested structure of Damaschun was constructed using the program Cerius^2.[22] This was used to visualize the projections required for transition moment averaging. For this purpose, it is convenient to define a set of orthogonal axes u, v, w, two of which lie in the same plane as the b and c axes of the unit cell. Then the a axis forms an angle with the third axis

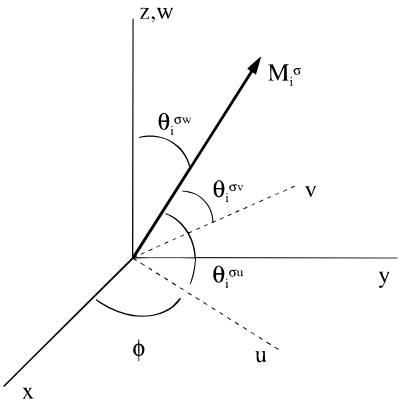

Figure 10. Projection of a transition moment M_i^σ from repeat unit σ onto the x axis using projection cosines and intermediate axes (u, v, w).

that is defined by the crystal structure, in which a and b are perpendicular to c, but a is not perpendicular to b. If two of the axes u, v, w are taken in the *xy* plane, the third is normal to it, and it is possible to model helical structures which are aligned either parallel or perpendicular to the water surface. Figure 10 shows how each transition moment is projected onto the u, v, w axes by the projection cosines, which are then projected onto the x axis. The contribution of one of the monomer repeating units designated by the index σ is

$$\begin{aligned} M_{x,i}{}^\sigma &= M_u{}^\sigma \cos\phi + M_v{}^\sigma \sin\phi \\ &= M_i \cos\theta_i{}^{\sigma u} \cos\phi + M_i \cos\theta_i{}^{\sigma v} \sin\phi \end{aligned} \tag{11}$$

which makes a contribution to the absorbance A_x as

$$\begin{aligned} A_{x,i}{}^\sigma &= \frac{1}{2} M_i{}^2 \{\cos^2\theta_i{}^{\sigma u} + \cos^2\theta_i{}^{\sigma v}\} \\ &= \frac{1}{2} M_i{}^2 \{1 - \cos^2\theta_i{}^{\sigma w}\} \end{aligned} \tag{12}$$

Adding the in-phase and out-of-phase contributions produces the contribution from one monomer unit

$$A_x{}^\sigma = \frac{1}{2} M_i{}^2 \{1 - \cos^2\theta_i{}^{\sigma w}\} + \frac{1}{2} M_j{}^2 \{1 - \cos^2\theta_j{}^{\sigma w}\} \tag{13}$$

The total absorbance is the average of the six individual contributions

$$A_x = \frac{1}{6} \sum_\sigma A_x{}^\sigma \tag{14}$$

allowing the absorbance to be calculated for any specific orientation of the helix. If the helix axis is perpendicular to the water surface, $A_x = 1.22M^2$, but if the helix axis is parallel to the water surface, the slightly larger result depends on the orientation of the helix, lying between $1.34M^2$ and $1.45M^2$, as shown in Table 1.

The experimental values of peak absorbances A/Γ are 0.017 ± 0.002 within one standard deviation at Γ_1 (data pooled from 0.64 to 0.91 mg/m^2) and 0.026 ± 0.003 at Γ_2 (data pooled from 1.46 to 3.1 mg/m^2). The ratio of these scaled absorbances is 1.5 ± 0.4. Although the error is quite large, the trend in Figure 8 clearly shows that the scaled absorbance at Γ_2 is significantly greater than it is at Γ_1. The ratio of twisted caterpillar to isotropic is $1{:}^2/_3 = 1.5$, suggesting that perhaps the isotropic case applies at Γ_1 and the twisted caterpillar at Γ_2. This would indicate that the structure at Γ_1 is

more three-dimensional than at Γ_2, in conflict with the expectation that the film thickness at Γ_2 be about twice that at Γ_1. Alternatively, a caterpillar structure is conceivable at Γ_1 and the more ordered helical structure with the helix axis parallel to the water surface at Γ_2, since the ratio would then lie between 1.34 and 1.45, consistent with the experimental value of 1.5 ± 0.4. An all-trans chain structure at Γ_2 appears to be ruled out since such a structure exposes the oxygen atoms to interaction with water, and the frequency of the asymmetric Si−O−Si stretching vibration is increased by 15 cm^{-1} at Γ_2 from that at Γ_1, indicating that the oxygen atoms are largely protected from interaction with water in the structure at Γ_2. This observation argues strongly for a helical structure at Γ_2, in which the oxygen atoms are somewhat interior to the helix and are protected from interaction with water. Additionally, most of the oxygen atoms are above the water when the helix is oriented with the helical axis parallel to the water surface. None of the other structures considered here is capable of providing similar protection. Certainly, the structure at Γ_2 must be more ordered than at Γ_1, since the experimentally determined ratio of scaled absorbances A/Γ is 1.5 ± 0.4, and Table 1 shows that the introduction of structure forces the ratio to exceed unity, whether the structure at Γ_1 is taken as isotropic or twisted caterpillar.

If the surface structure at Γ_2 consisted of two or more layers of poly(dimethylsiloxane) molecules, the oxygen atoms in the upper layer or layers would also be denied access to subphase liquid water, and the 1020 cm^{-1} band would dominate the spectrum in the 1000 cm^{-1} region. If the layer were thick enough, the incident infrared radiation would not penetrate to the layer in contact with subphase liquid water, and the 1005 cm^{-1} band would vanish from the reflectance absorption spectrum. The fact that the 1005 cm^{-1} band survives in all spectra obtained shows that the incident infrared radiation penetrates at least as far as the oxygen atoms in contact with liquid water. This suggests that the film is not very thick at Γ_2 and further suggests that there is some mechanism that removes most of the oxygen atoms from contact with liquid water in the phase stable at this surface concentration. Furthermore, if two or more layers were present at Γ_2, at least one of the layers would have to exhibit some structure in order to accommodate the experimental observation of 1.5 ± 0.4 for the ratio of scaled absorbances A/Γ for the symmetric methyl deformation at 1264 cm^{-1}. While these experimental observations are not sufficient to define the film structure at Γ_2, none are inconsistent with the horizontal helix. Taken together, these observations suggest that the film at Γ_2 may well be too thin to be consistent with multilayer structures stable at large surface concentrations, though the data obtained do not allow a definitive depth profile of the surface layer. Thus, these observations favor some structure at Γ_2, such as the horizontal helix, but do not definitively rule out other possible interpretations.

Conclusion

Fluorescence microscopy and external reflectance infrared spectroscopy results are presented that characterize the behavior of poly(dimethylsiloxane) films at the air−water interface in the plateau region near 9 mN/m between surface concentrations of approximately 0.75 and 1.6 mg/m^2. The fluorescence microscopy results show bright domains and dark domains that persist over the concentration range, the relative amounts of which are consistent with a surface phase transition within experimental error. The external infrared reflectance results show that the phase stable at the higher surface concentration is one in which the oxygen atoms in poly(dimethylsiloxane) are largely excluded from contact with the liquid water substrate, while the oxygen atoms are in intimate contact with water in the structure stable at the lower surface concentration. The ratio of the scaled reflected absorbance for the symmetric methyl deformation at 1264 cm^{-1} to the surface concentration is not constant over the concentration range. The ratio of absorbance at the high concentration limit to that of the low concentration limit is 1.5 ± 0.4, consistent with reflected absorbance ratios predicted for several possible ordered poly(dimethylsiloxane) structures. Stable structures consistent with the observed spectra at the concentration limits are the twisted caterpillar, or two-dimensional random coil, stable at the lower limit, and possibly a helical structure which has the helix axis parallel to the air−water interface at the upper limiting surface concentration.

Acknowledgment. This work was supported by the National Science Foundation Materials Research Laboratory at the University of Massachusetts and a grant from American Chemical Society, Petroleum Research Fund, No. 30573-AC7.

References and Notes

(1) Fox, H. W.; Taylor, P. W.; Zisman, W. A. *Ind. Eng. Chem.* **1947**, 1401.
(2) Garrett, W. D.; Zisman, W. A. *J. Phys. Chem.* **1970**, *74*, 1796.
(3) Granick, S.; Clarson, S. J.; Formoy, T. R.; Semlyen, J. A. *Polymer* **1985**, *26*, 925.
(4) Lee, L. T.; Mann, E. K.; Langevin, D.; Farnoux, B. *Langmuir* **1991**, *7*, 3076.
(5) Lee, L. T.; Langevin, D.; Mann, E. K.; Farnoux, B. *Physica B* **1994**, *198*, 83.
(6) Lenk, T. J.; Lee, D. H. T.; Koberstein, J. T. *Langmuir* **1994**, *10*, 1857.
(7) Mann, E. K.; Langevin, D. *Langmuir* **1991**, *7*, 1112.
(8) Mann, E. K.; Henon, S.; Langevin, D.; Meunier, J. *J. Phys. II, France* **1992**, *2*, 1683.
(9) Mann, E. K.; Langevin, D.; Henon, S.; Meunier, J.; Lee, L. T. *Ber. Bunsen-Ges. Phys. Chem.* **1994**, *98*, 519.
(10) Noll, W.; Steinbach, H.; Sucker, C. *J. Polym. Sci., Part C* **1971**, *34*, 123.
(11) McConnell, H. M. *Annu. Rev. Phys. Chem.* **1991**, *42*, 171.
(12) Mohwald, H. *Annu. Rev. Phys. Chem.* **1990**, *41*, 441.
(13) Weis, R. M. *Chem. Phys. Lipids* **1991**, *57*, 227.
(14) Smith, A. L. *Spectrochim. Acta* **1960**, *16*, 87.
(15) Wright, N.; Hunter, M. J. *J. Am. Chem. Soc.* **1947**, *69*, 803.
(16) Wilmshurst, J. K. *J. Chem. Phys.* **1957**, *26*, 426.
(17) Konopka, R.; Stojczyk, B. *Acta Phys. Pol.* **1971**, *A40*, 537.
(18) Bauer, R.; Magat, M. *J. Phys. Radium* **1938**, *9*, 319.
(19) Allerhand, A.; Schleyer, P. v. R. *J. Am. Chem. Soc.* **1963**, *85*, 371.
(20) Zbinden, R. *Infrared Spectroscopy of High Polymers*; Academic Press, Inc.: New York, 1964.
(21) Damaschun, V. G. *Kolloid-Z., Z. Polym.* **1962**, *180*, 65.
(22) This program was developed by Molecular Simulations Inc.

MA9611228